Princeton Plasma Physics Laboratory

PPPL- 4679

PPPL- 4679

Particle-In-Cell Simulation of Ion Beam Neutralization by a Tenuous Background Plasma

William Berdanier and Igor Kaganovich

September, 2011

Prepared for the U.S. Department of Energy under Contract DE-AC02-09CH11466.

Particle-In-Cell Simulation of Ion Beam Neutralization by a Tenuous Background Plasma

William Berdanier
Department of Physics, The University of Texas at Austin, Austin, Texas 78712, and National Undergraduate Fellowship Program, Princeton Plasma Physics Laboratory, James Forrestal Campus, Princeton, New Jersey 08543

Advisor: Igor Kaganovich
Princeton Plasma Physics Laboratory, James Forrestal Campus, Princeton, New Jersey 08543

(Dated: August 12, 2011)

The neutralization and focusing of intense charged particle beam pulses by electrons forms the basis for a wide range of applications for accelerators, heavy ion fusion, and astrophysics. For intense ion beam pulses, a background plasma can be used to effectively neutralize the beam charge and current, thereby neutralizing the self-fields. We show that even a tenuous background plasma with a small relative density can achieve high neutralization. Using the Large Scale Plasma (LSP) particle-in-cell code, the interaction of an intense ion beam with an underdense plasma was simulated. It was shown that if the total plasma electron charge is comparable to the beam charge, electron emitters are necessary for effective neutralization. These are not needed if the plasma volume is large. A variety of plasma densities was investigated, including the case of emitters without plasma, which did not effectively neutralize the beam. Over 95% neutralization was found for even very tenuous background plasma, in agreement with earlier analytical studies.

BACKGROUND

Neutralization and focusing of intense charge particle beams by background plasma form the basis for a variety of applications to high-energy accelerators and colliders, astrophysics, inertial confinement fusion, in particular, fast ignition and heavy ion fusion, magnetic fusion based on field-reversed configurations fueled by energetic ion beams, the physics of solar flares, high-intensity high-energy particle beam propagation in the atmosphere and outer-space plasmas, as well as basic plasma physics phenomena. For instance, one of the modern approaches to ion beam compression for heavy ion fusion applications is to use a dense background plasma, which charge neutralizes the ion charge bunch, and hence facilitates compression of the charge bunch against strong space-charge forces. [**?**]

The equation governing the evolution of the beam radius r_b is

$$\frac{d^2 r_b}{dz^2} = \frac{Q}{r_b} + \frac{\varepsilon^2}{r_b^3}, \tag{1}$$

where cylindrical coordinates and azimuthal symmetry are assumed. The first term is deemed the perveance term, and the second is called the emittance term. Ion beams used for heavy ion fusion applications are space-charge perveance dominated, i.e., the space-charge potential energy is large compared with the ion beam temperature, or equivalently, the perveance term in the equation for the beam envelope is large compared with the emittance term. These perveance-dominated scenarios will be the focus of this paper, although the results hold for more general applications.

Neglecting the permittance term, Eq. 1 can be integrated (by multiplying by r_b' and integrating) to obtain

$$\left(\frac{dr_b}{dz}\right)^2 = {r_i'}^2 + 2Q\ln\left(\frac{r_b}{r_i}\right), \tag{2}$$

where $r_i' = \frac{dr_b}{dz}|_i$ is the initial angle of beam convergence, and r_i is the initial radius of the beam. For heavy ion fusion applications, the beam pulse is focused over distances of 15 m, corresponding to the reactor chamber size; during focusing, an initial beam radius of 12 cm is reduced to a spot radius of about 1 mm or less. For this weak ballistic focusing, the beam space charge has to be neutralized well enough so that the beam convergence angle is not affected by the self-fields of the beam pulse during the drift, i.e., from Eq. 2 it follows that the degree of charge neutralization, f, should satisfy the following condition:

$$2(1-f)Q\ln\left(\frac{r_i}{r_f}\right) \ll {r_i'}^2. \tag{3}$$

Some estimates of these parameters are available from the Neutralized Drift Compression eXperimentI (NDCX-I), a collaborative heavy-ion inertial confinement fusion experiment at Lawrence Berkeley National Lab. Substituting these, namely $r_i \sim 10^{-2}, Q \sim 10^{-3}$, and $\frac{r_i}{r_f} \sim 10$, into Eq. 3, we obtain that the degree of neutralization should satisfy $(1-f) \ll 10^{-2}$, so the neutralization must be better than 99%. That is, for a heavy ion fusion driver, the beam self-field potential is initially of order 10 kV, whereas the self-field potential after neutralization should be less than 100 V.

It has been shown in previous studies that the only way presently known to achieve this high level of charge neutralization is to ballistically propagate the beam through a background plasma. The question experimentally becomes, how strong need the background plasma be in order to neutralize the beam? This is the basis of the present investigation, which finds that even a quite tenuous plasma ($n_p \ll n_b$) can effectively neutralize the ion beam.

THEORY

It is useful to discuss the concept of particle-in-cell simulation, how it functions (in brief), and also introduce some analytic results with regards to the neutralization of fixed-shape beams by background volumetric plasma.

PIC Codes

For this investigation, I used the Large Scale Plasma (LSP) suite of Particle-In-Cell (PIC) code, commercially available from Alliant Techsystems, LLC. In short, PIC codes work by representing a background density with super-particles, each of which are point particles that represent a chunk of density, in a gridded region of space. The amount of real particles that each super-particle represents depends on the fineness of the grid (the number of cells per dimension for a given region), the density of the region, and the number of particles per cell. For example, a high density, coarse grid, low particle-per-cell count simulation would suffer from numerical noise, since each super-particle would have to represent a large density. Statistical noise scales as $1/\sqrt{n}$, where n is the number of particles per cell, so the noise-to-signal ratio scales as $n^{-3/2}$. Therefore, for low n, the ratio is large, and thus the signal is obscured. Further, this high noise leads to some non-physical effects, such as heating and large, fluctuating fields. It is wise to carefully manage these three numbers. As a rule of thumb, grid spacing Δx and time step Δt must obey:

$$\begin{aligned}\Delta x &\leq 3.4\lambda_D \\ \Delta t &\leq q2\omega_{pe}^{-1}.\end{aligned}$$

At the start of a PIC simulation, the user has defined some initial seeding for the initial particles. Particles can subsequently be created according to many models, such as background plasma, particle injection, and secondary emission (Child-Langmuir-limited) to name a few. A characteristic time interval for the simulation is defined by the user, but can be automatically interpolated by LSP as well (the Courant limit). The time interval must be small enough that the forces upon all particles do not change very much within the interval. This implies that between time steps, the distance traveled by particles is approximately kinematic in nature (i.e. not an integral, but simply an algebraic function of velocity and force over mass). Two solver methods are generally used to calculate particle trajectories: the leapfrog method, which is explicit, and the Boris scheme, which is implicit. The act of advancing the particles in a PIC simulation takes the majority of the computation time, as the particle movers must be evaluated for every particle in the simulation (which, although each particle represents a large density, contain many particles, sometimes on the order of 10^6 or 10^7).

Leapfrog Method

Leapfrog methods in general are named such because the calculation of the particle velocities is an average of the positions at the previous step and at the next step, and the forces are calculated at the previous velocity and the next velocity. Thus, the force calculations are halfway in between two position steps, and this is interpolated back to find the next position. Mathematically:

$$\begin{aligned}\frac{\mathbf{x}_{k+1}-\mathbf{x}_k}{\Delta t} &= \mathbf{v}_{k+1/2} \\ \frac{\mathbf{v}_{k+1/2}-\mathbf{v}_{k-1/2}}{\Delta t} &= \frac{q}{m}\Big(\mathbf{E}_k + \frac{\mathbf{v}_{k+1/2}+\mathbf{v}_{k-1/2}}{2}\times\mathbf{B}_k\Big)\end{aligned}$$

where the subscript k refers to quantities from the previous time step, $k+1$ to the updated quantities ($t_{k_1} = t_k + \Delta t$), and velocities are calculated in between timesteps.

Boris Scheme

The Boris scheme, on the other hand, uses the setup:

$$\begin{aligned}\mathbf{x}_{k+1} &= \mathbf{x}_k + \Delta t\mathbf{v}_{k+1/2} \\ \mathbf{v}_{k+1/2} &= \mathbf{u}' + q'\mathbf{E}_k\end{aligned}$$

with

$$\begin{aligned}\mathbf{u}' &= \mathbf{u} + (\mathbf{u} + (\mathbf{u}\times\mathbf{h}))\times\mathbf{s} \\ \mathbf{u} &= \mathbf{v}_{k-1/2} + q'\mathbf{E}_k \\ \mathbf{h} &= q'\mathbf{B}_k \\ \mathbf{s} &= 2\mathbf{h}/(1+\mathbf{h}\cdot\mathbf{h}) \\ q' &= \frac{\Delta t}{2q/m}.\end{aligned}$$

Field Solvers

In order to move the particles, the fields must first be solved. Three methods are common for solving Maxwell's equations: Finite Difference Methods (FDM), Finite Element Methods (FEM), and spectral methods.

In FDM, the continuous domain is divided into a grid on which electric and magnetic fields are calculated. Derivatives are approximated as the differences between neighboring grid-point values and so the partial differential equations become algebraic.

In FEM, the continuous domain is divided into a discrete mesh of elements. The partial differential equations are treated as an eigenvalue problem and a trial solution is first calculated using basis functions that are localized in each element. The solution is then optimized until the desired accuracy is reached.

Some spectral methods are also available, such as using a fast Fourier transform on the partial differential equations to transform to an eigenvalue problem, but with global basis functions instead. Importantly, here the domain is not discretized. A trial function is again used.

Approximate System of Equations

Here we make the assumptions that all quantities are stationary in the reference frame of the beam, i.e. all quantities depend on t and z exclusively through the combination

$$\zeta = v_b t - z. \tag{4}$$

We carry out the analysis in the lab frame of reference, where

$$\left(\frac{\partial}{\partial t}\right)_z = v_b \frac{\partial}{\partial \zeta} \tag{5}$$

$$\left(\frac{\partial}{\partial z}\right)_t = -\frac{\partial}{\partial \zeta}. \tag{6}$$

We further assume that the beam is long and cylindrically symmetric, that is, $l_b \gg v_b/\omega_p$, $l_b \gg r_b$, where $\omega_p = \sqrt{4\pi e^2 n_e/m}$ is the electron plasma frequency. The electron fluid equations and Maxwell's equations fully describe the beam propagation. The fluid equations consist of the continuity equation

$$\frac{\partial n_e}{\partial t} + \nabla \cdot n_e \mathbf{v}_e = 0 \tag{7}$$

and the force balance equation

$$\frac{\partial \mathbf{p}_e}{\partial t} + (\mathbf{v}_e \cdot \nabla)\mathbf{p}_e = -e\Big(\mathbf{E} + \frac{1}{c}\mathbf{v}_e \times \mathbf{B}\Big), \tag{8}$$

with $-e$ the electron charge, m the electron rest mass, $\mathbf{v}_e$ the electron flow velocity, $\mathbf{p}_e = \gamma_e m \mathbf{v}_e$ the electron momentum, and $\gamma_e = (1 - v_e^2/c^2)$ is the relativistic mass factor. Maxwell's equations in this scenario read

$$\nabla \times \mathbf{B} = \frac{4\pi e}{c}(Z_b n_b \mathbf{v}_b - n_e \mathbf{v}_e) + \frac{1}{c}\frac{\partial \mathbf{E}}{\partial t} \tag{9}$$

$$\nabla \times \mathbf{E} = -\frac{1}{c}\frac{\partial \mathbf{B}}{\partial t}, \tag{10}$$

with $\mathbf{v}_b$ the ion beam velocity, n_e and n_b the number densities of the plasma electrons and the beam ions respectively, and Z_b is the beam ions' charge state.

We can simplify this system by making use of the conservation of generalized vorticity, $\mathbf{\Omega} = \nabla \times \mathbf{p}_e - e\mathbf{B}/c$. Taking the curl of Eq. 8 and making use of Eq. 10,

$$\frac{\partial \mathbf{\Omega}}{\partial t} - \nabla \times (\mathbf{v}_e \times \mathbf{\Omega}) = 0, \tag{11}$$

which can be rewritten

$$\frac{\partial \mathbf{\Omega}}{\partial t} + (\mathbf{v}_e \cdot \nabla)\mathbf{\Omega} = -\mathbf{\Omega}(\nabla \cdot \mathbf{v}_e) + (\mathbf{\Omega} \cdot \nabla)\mathbf{v}_e. \tag{12}$$

It can be shown that if $\mathbf{\Omega} = 0$ everywhere at some initial time, then it continues to vanish at all subsequent times. We will only need examine those situations in which this is the case. Thus, the magnetic field is related to the electron flow velocity as

$$\mathbf{B} = \frac{c}{e}\nabla \times \mathbf{p}_e, \tag{13}$$

which can be substituted into Eq. 8 to become

$$\frac{\partial \mathbf{p}_e}{\partial t} + \nabla K_e = -e\mathbf{E} \tag{14}$$

with $K_e = \gamma_e mc^2$ the electron energy.

Previous results were exact. We now make use of the approximations outlined at the beginning of this section. We can find the electron flow velocity by substituting into Ampere's law, yielding

$$-\frac{1}{r}\frac{\partial}{\partial r}\Big[r\Big(\frac{\partial p_{ez}}{\partial r} + \frac{\partial p_{er}}{\partial \zeta}\Big)\Big] = \frac{4\pi e^2}{c^2}(Z_b n_b v_b - n_e v_{ez}) + \frac{e v_b}{c^2}\frac{\partial E_z}{\partial \zeta}, \tag{15}$$

which reduces under the long-beam assumption to

$$-\frac{1}{r}\frac{\partial}{\partial r}\Big[r\Big(\frac{\partial p_{ez}}{\partial r}\Big)\Big] = \frac{4\pi e^2}{c^2}(Z_b n_b v_{bz} - n_e v_{ez}). \tag{16}$$

Both the electron and ion radial velocities are negligibly small compared to their longitudinal counterparts, which is reflected by the above expression. This also shows that the degree of neutralization is determined by the ratio of the beam radius r_b to the skin depth $\delta = c/\omega_p$. In the case at hand, $r_b \ll c/\omega_p$, so the current is not neutralized, and the electron longitudinal velocity is determined entirely by the ion beam current and does not depend on the plasma density.

The radial electron flow velocity can be determined from the electron continuity equation (Eq. 7),

$$v_{er} = -\frac{1}{r n_e}\frac{\partial}{\partial \zeta}\int_0^r [n_e(v_b - v_{ez}) - n_p v_b] r dr \tag{17}$$

where n_p is the uniform background plasma density with no beam present. If quasineutrality is assumed, then $n_e(v_b-v_{ez})-n_pv_b=(n_e-n_p)v_b-n_ev_{ez}=Z_bn_bv_b-n_ev_{ez}\equiv j_z/e$, the above equation simplifies to become

$$v_{er}=-\frac{1}{ern_e}\frac{\partial}{\partial\zeta}\int_0^r j_z r dr \tag{18}$$

with $j_z=e(Z_bn_bv_b-n_ev_{ez})$ the longitudinal current. Substituting these expressions for v_{er} and v_{ez} into Eq. 14 then yields the electric field

$$\mathbf{E}=-\frac{1}{e}\Big(v_b\frac{\partial\mathbf{p}_e}{\partial\zeta}+\boldsymbol{\nabla}K_e\Big). \tag{19}$$

Substituting into Eq. 13 yields the azimuthal magnetic field

$$B=-\frac{c}{e}\Big(\frac{\partial p_{ez}}{\partial r}+\frac{\partial p_{er}}{\partial\zeta}\Big). \tag{20}$$

Finally, the degree of charge neutralization can be estimated from Poisson's equation,

$$\rho=e(Z_bn_b-n_e)=\frac{1}{4\pi}\boldsymbol{\nabla}\cdot\mathbf{E}. \tag{21}$$

It can be shown that the maximum deviation from quasineutrality occurs when $r_b\sim c/\omega_p$, and

$$|\rho|\lesssim e\beta_b^2Z_bn_b. \tag{22}$$

Thus for long ion beam pulses, $|\rho|/eZ_bn_b\ll 1$ and there is nearly complete charge neutralization. For calculational purposes we can assume complete charge neutrality,

$$n_e=Z_bn_b+n_p \tag{23}$$

and treat deviations as perturbations.

The radial force acting on the beam ions can also be determined in terms of the electron flow velocity. Substituting above relations for $\mathbf{E}$ and B into the ion force equation yields

$$F_r=eZ_b\Big(E_r-\frac{1}{c}v_bB\Big)=-Z_b\frac{\partial}{\partial r}(K_e-v_bp_{ez}). \tag{24}$$

Since the radial flow velocity is slow compared to the longitudinal flow velocity, it can be neglected, yielding

$$F_r=Z_bm\gamma_e^3(v_b-v_{ez})\frac{\partial}{\partial r}v_{ez}. \tag{25}$$

PROCEDURE

My LSP simulations consisted of two geometries, two-dimensional Cartesian XZ slab and two-dimensional cylindrical RZ slice. The explicit particle mover and field solver were used. I will give the parameters for these geometries separately.

Cartesian XZ Geometry

This consisted of a box, $-13\le x\le 13$ cm and $0\le z\le 100$ cm. The grid was 808 z-cells by 104 x-cells. This was split into 32 domains (one domain corresponds to one processor), equally spaced in the z-direction. Background plasma filled the chamber at varying densities, namely 2.4×10^{10} per cm^{3}and 8.0×10^9 per cm^3, corresponding to a beam density to plasma density ratio of 5 and 15, respectively. A beam of carbon ions was injected into the plasma at a fixed distribution (these particles were not simulated, as they were assumed to be so massive as to be immobile during the simulation). This distribution was a Gaussian profile of two variables, of width 3 cm in the x direction and 30 cm in the z direction. The beam energy was measured in units of $\gamma\beta=v/c\sqrt{1-v^2/c^2}$, and in these units had the value of 0.3575118. The beam propagation direction was the z-direction, and took 15 nanoseconds to traverse the meter-long simulation (at 0 ns, the beam had not entered, and at 15 ns, it had fully exited). The time step was 0.01 ns. The walls were allowed to emit electrons due to secondary emission, that is, the beam pulse could rip electrons off the walls so as to facilitate beam neutralization. For all electron species, 17 particles were initiated per x-cell, while 5 were initiated per z-cell, giving an initial density of 75 particles per cell. Symmetry along y was assumed; therefore, the number of particles indeed scaled as the simple product of particles per x-cell by particles per z-cell. The total number of particles increased as the simulation progressed, since particles were emitted, but stayed on the order of 7-8$\times10^6$ for the duration of the simulation.

Three other cases were explored: one in which the field-stress emission could only occur from the sides of the chamber, one in which a region of dense plasma (1.2×10^{12} per cm^3) 2 cm thick was placed on the sides and front of the chamber, and one in which the dense plasma was only present on the sides. These cases were explored for both plasma densities.

Cylindrical RZ Geometry

The cylindrical geometry was explored primarily because it had more physical significance to real experiments (there are almost no slab-geometry plasma devices, while cylindrical plasma devices are extremely common). Almost all parameters were the same; I will only recount the ones that changed. First, the dimensions on r were different than those of x, since azimuthal symmetry is assumed, and r cannot take on a negative value. Thus, $0 \leq r \leq 13$ cm. The number of r-cells remained the same as the number of x-cells, however, so the grid spacing in the r direction halved. Thus, the grid spacing in both directions was 0.125 cm. This geometry was explored for all cases above. The largest difference comes in the number of particles; in Cartesian geometry, the number of particles scales as a constant, while in cylindrical geometry, the number of particles scales as r, so the number of particles in the simulation was much higher. The initial seeding was 7×10^6 particles, but by the end of the simulation the number had risen to almost 1.2×10^7.

RESULTS

I explored several cases, as discussed above, for beam density to plasma density ratios of $n_b/n_p \in \{5, 15, 30\}$. I also explored the case of just having emitting walls, and just having background tenuous plasma, for the purposes of demonstrating that the requisite high degree of neutralization is only achievable with both electron sources at once.

Naked Beam Fields

For comparison with later neutralized simulations, it is useful to look at the strength and shape of the electric and magnetic fields from the beam pulse propagating in isolation (through vacuum). The electric field is of order $E_r \sim 250$ kV/cm:

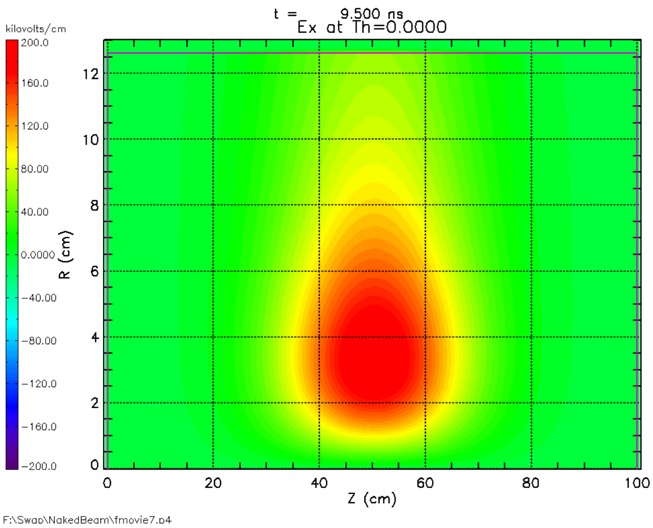

and the magnetic field is of order $B_\theta \sim 200$ G:

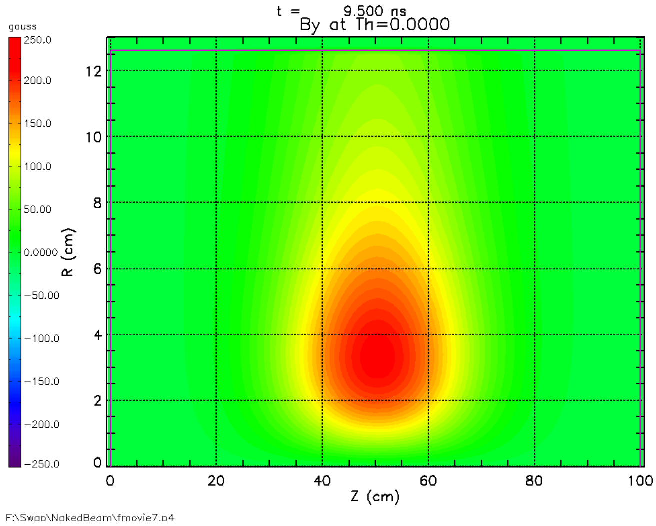

Neutralization by Emitters Alone

It was found that neutralization by emitters alone on the side walls was ineffective. This is due to two effects: the acceleration of charges from the wall to the center of the chamber (where the ion beam pulse lies) gives them a high thermal energy, leading to high thermal noise, and it also give them a tendency to overshoot the center and simply oscillate back and forth through the ion pulse without effectively neutralizing. Taking a slice along the z-direction and slightly off axis to negate numerical effects (at $r = 2$),

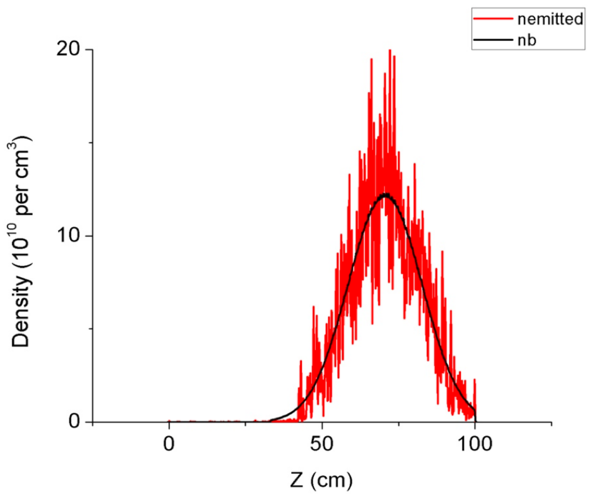

Clearly, the distribution appears to match relatively well. However, comparing the electric field contour plot, we see that strong fields still exist, even as the beam pulse is near exit of the simulation region:

These electric fields are only 80% neutralized, indicating that the neutralization does not meet the high level required for ICF applications.

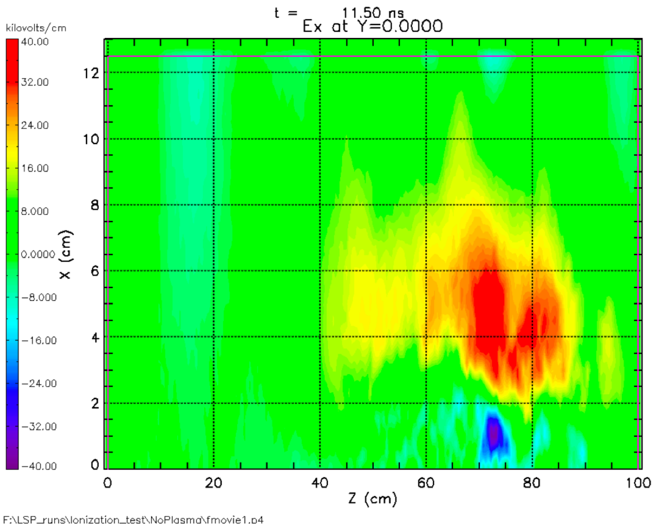

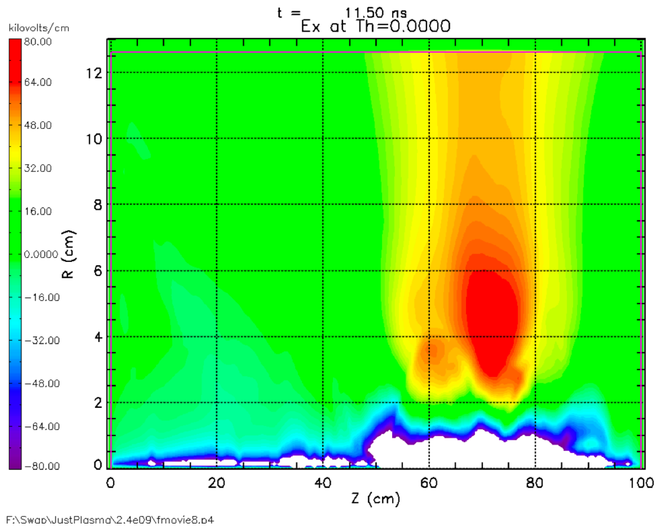

Neutralization by Tenuous Background Plasma Alone

It was found that neutralization by a tenuous background plasma alone has two pitfalls: large fields are created within the plasma as electrons are stripped to neutralize the beam, and if the plasma is too tenuous, then not enough charge can be accumulated in the length scale available to experiments. To demonstrate the first point, I simulated the propagation of an ion beam pulse through a background plasma with $n_b/n_p = 5$:

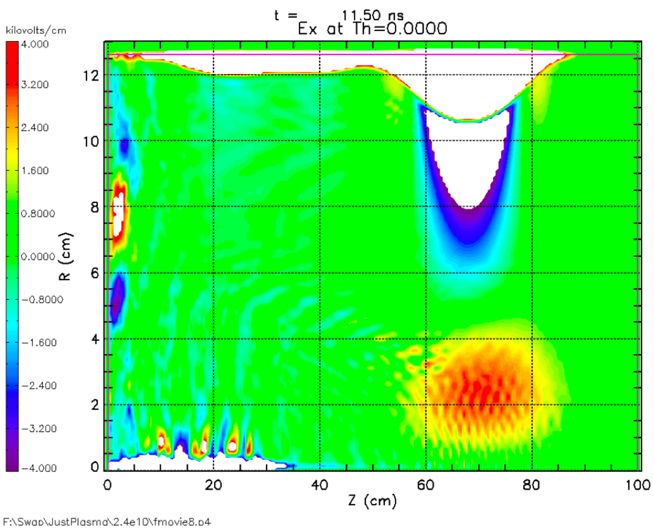

While neutralization of the pulse itself is quite high - the self-electric field from the pulse is of order 4 kV/cm, which is 98% lower than the unneutralized fields - large plasma fields, of order 70 kV/cm, are created at the edge of the plasma, where there is an overabundance of positive ions.

To demonstrate the second point, I simulated the propagation of an ion beam pulse through a background plasma with $n_b/n_p = 5$:

It is most effective to utilize a hybrid neutralization scheme that employs both a source of emitted electrons and a tenuous background plasma. I will explore both a case in which emission is allowed via Child-Langmuir limited current flow, in which electrons can be emitted from the side walls of the chamber if the sides experience a field greater than 0.001 V/cm (i.e. electrons will be emitted in response to virtually any field), and the case of having a region of dense plasma on the walls. This dense plasma region is two centimeters thick, that is, instantiated over $11 \leq r \leq 13$ cm, and has a gaussian profile of maximum $1.2{\times}10^{11}$ per cm^3 and a characteristic decay scale of 0.4 to 0.5 cm depending on the plasma density (the plasma density and dense region density exactly match at the $r = 11$ boundary). By characteristic length scale, I mean σ_1 in the expression $f = \exp[x^2/\sigma_1^2]$. A gaussian profile was used for numerical purposes; in previous simulations, numerical noise was caused by having a flat-top profile with a steep wall of density between the dense region and tenuous region.

Neutralization by Emitters and Tenuous Plasma

Turning first to a case that is quite tenuous by experimental standards, in which $n_b/n_p = 5$, we can see the general process of neutralization below. The beam density n_b is on the left, the plasma electron density n_p is in the center, and the emitted electron density n_{emitted} is on the right.

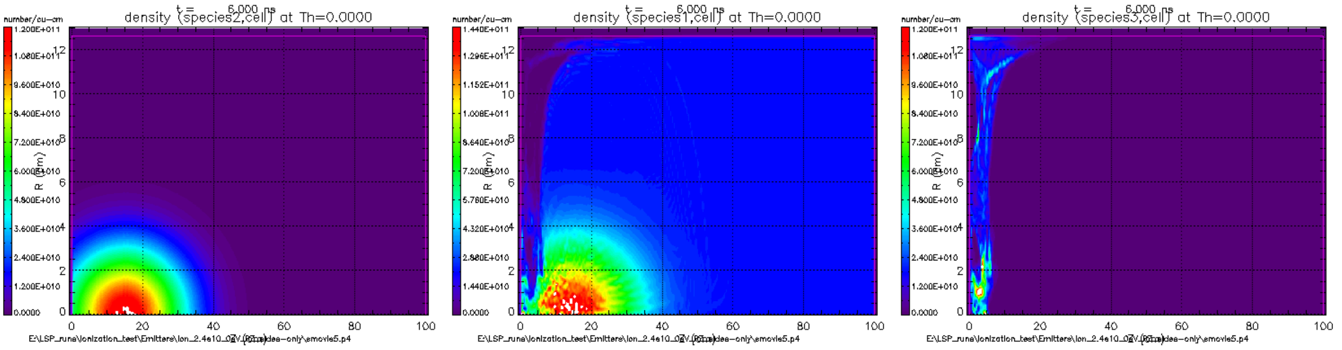

$t = 6.0$ ns.

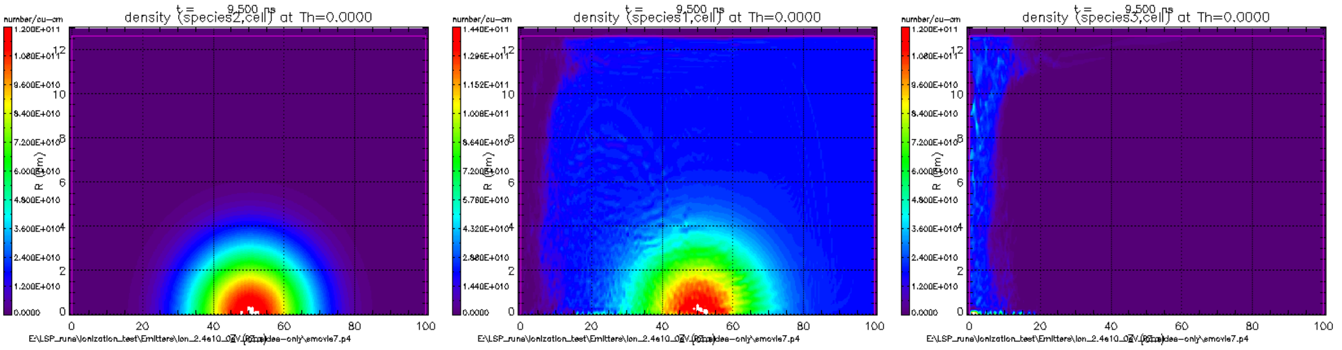

$t = 9.5$ ns.

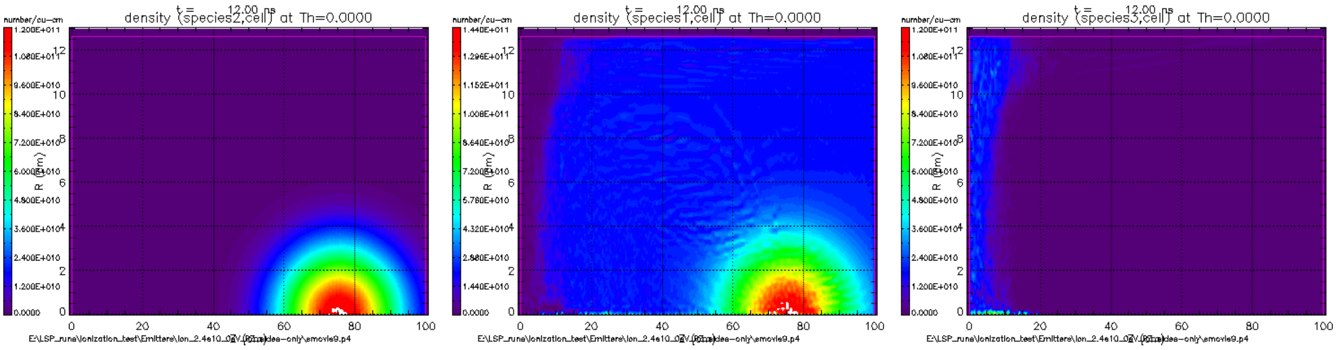

$t = 12.0$ ns.

As the ion beam enters, it sucks electrons from the background plasma. This leaves a hole in the plasma where those electrons were before, which has a strong electric field since many now unneutralized ions fill the region. These ions' field pulls electrons from the walls, as shown in the first slide. The electrons fill the gap, and contribute to the neutralization. As the ion pulse propagates, it sucks in electrons from the front, while, since the current neutralization is poor, the electrons move more slowly than the ions (i.e. they are not accelerated to the same speed as the ions) and thus eventually are ejected out the back of the pulse. Thus the process of flushing electrons continues until all the emitted electrons have been replaced by plasma electrons. While the length scale of the emitted electrons being completely flushed depends on the background plasma density, the general process is the same.

Taking a z-slice along $r = 2$ as before, shortly after the beam pulse has fully entered the plasma ($t = 7.5$ ns),

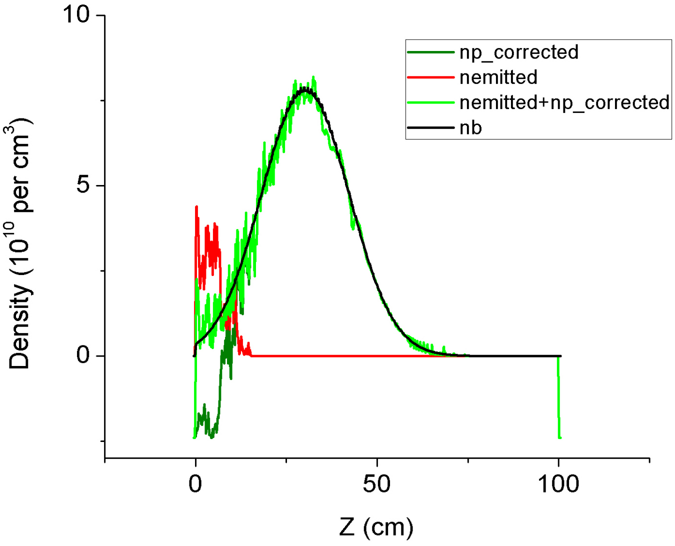

In these graphs, n_p has been shifted down by the background plasma density so that it represents the negative of the net charge in the background plasma. The sum of this net difference from equilibrium and the emitted electrons should balance the ion beam pulse. We can immediately see that the plasma and emitters combination has neutralized the ion beam pulse to high level, with most of the neutralization being done by the plasma, even at this early stage in which the beam pulse has barely fully entered the plasma. This high neutralization continues, and the emitted electrons have been completely flushed by the end of the simulation, and their role is to only fill the gap in plasma electrons left by their moving to neutralize the ion beam:

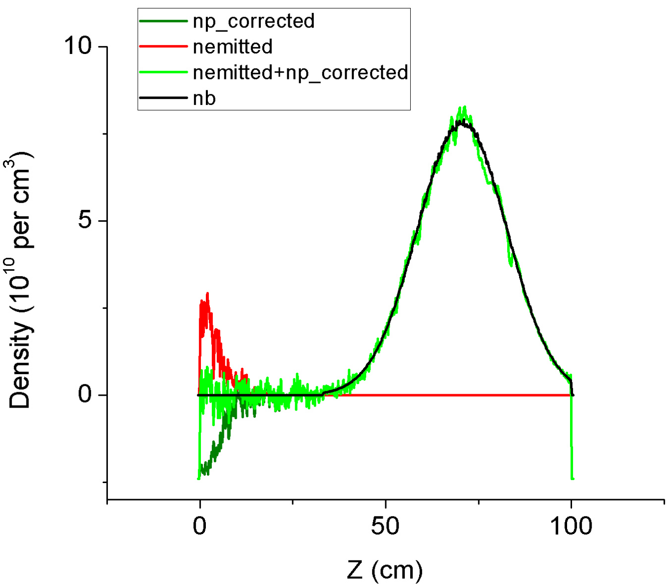

Taking an r slice can also be telling, since it could, at this point, be that the neutralization is good near axis but bad farther away. Taking an r-slice at $z = 30$ cm, $t = 7.50$ ns and $z = 70$ cm, $t = 11.50$ ns, at the center of the beam pulse in both cases:

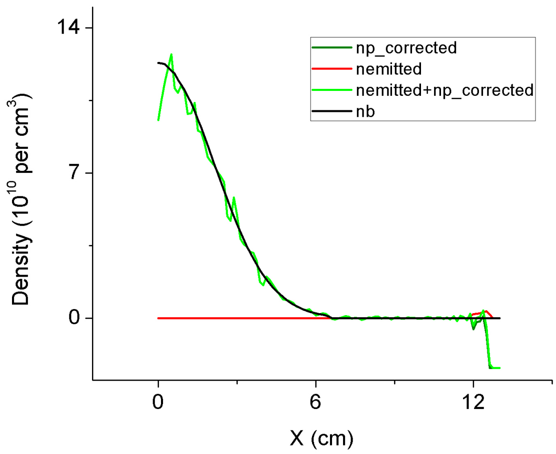

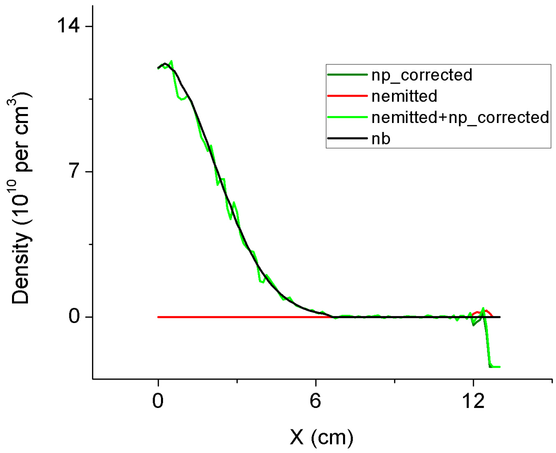

Ignoring axis effects, the neutralization is quite good and performed in this direction entirely by the plasma electrons. This is because the emitted electrons are only needed for the region $0 \le z \le 10$ cm.

Further, the electric fields are neutralized to less than 98% of the naked beam levels:

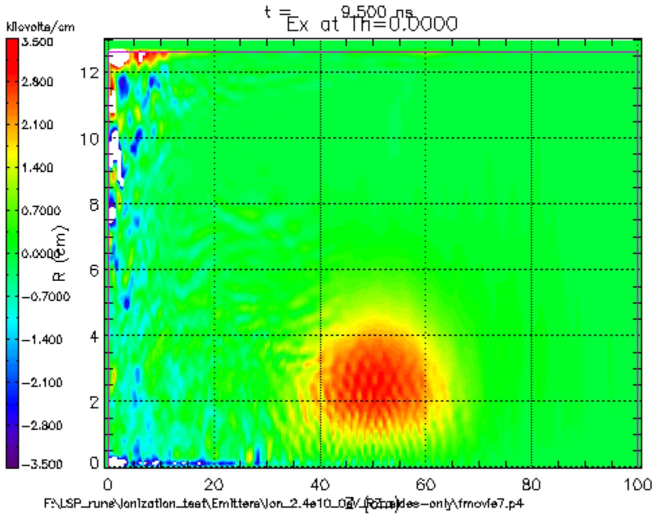

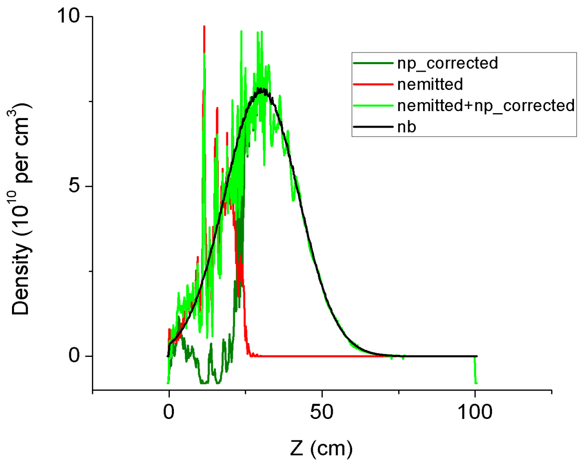

Thus we have conclusively shown excellent charge neutralization by an underdense plasma and emitters. However, the other cases drive home the point. It is also of interest to discuss the level of current neutralization:

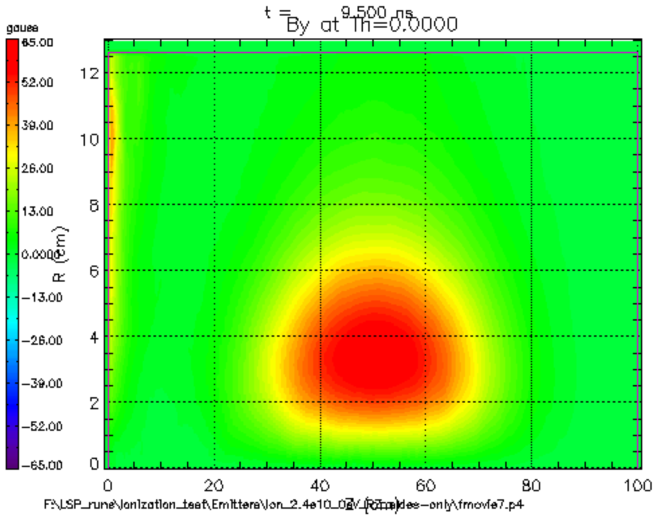

This B field is of order 65 G, which is only 75% neutralization from the naked beam field of 200 G. This is all right, though, since having a net current leads to a focusing self-magnetic force, and for compression/ICF schemes, compression is desirable. It should be noted that the sign of the field is the same as in the naked beam case, meaning that the net current points in the same direction and that therefore the ions must be moving faster than the neutralizing electrons, which is in agreement with the flushing effect noted earlier.

Now, I increased the beam density to plasma density ratio to $n_b/n_p = 15$. High neutralization was found in this case as well:

The reliance on emitted electrons is higher, as expected, and they are flushed on a length scale of 25 cm instead of 5 to 10 cm as in the previous case. Still, by the simulation's end, they have been entirely flushed again and the neutralization is done entirely by the plasma electrons:

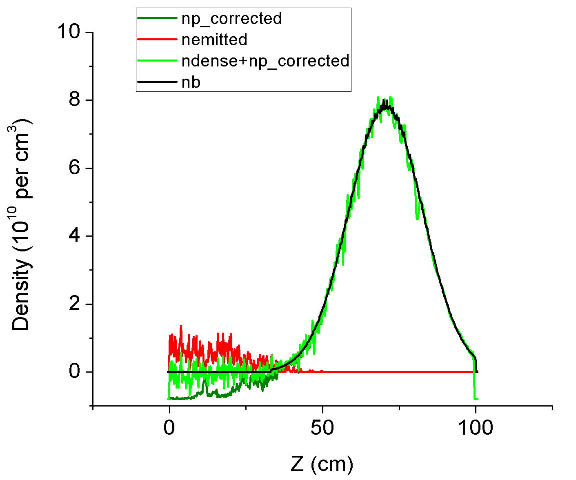

Comparing the electric field contours:

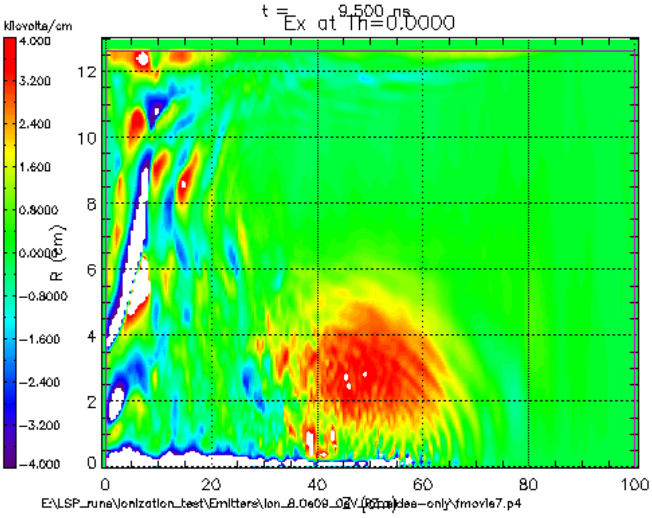

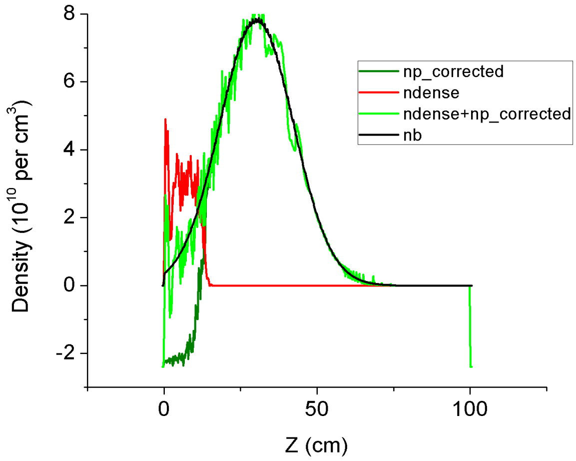

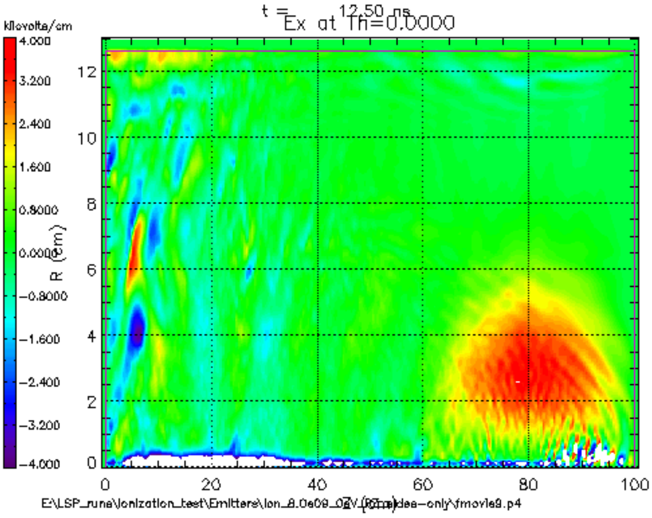

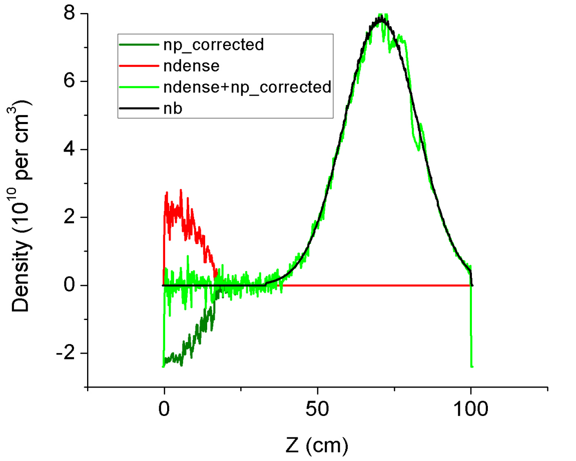

We see that as the beam relies on emitted electrons for neutralization purposes, the signal becomes more noisy, as reflected in the density plots. However, the order of the electric fields is about 4 kV/cm, which is 98% lower than that of the naked beam fields.

Neutralization by Dense Plasma on Walls and Tenuous Plasma Background

I found this scenario to be effectively identical to that of emitters, for both plasma density ratios discussed so far. This scenario, with a dense plasma region on the walls, is perhaps more physical, since experimentally there are many means with which to bolster the plasma density near the walls of a container.

Reliance on the emitted electrons appears to occur over the same length scale - about 10 cm. The only difference in this simulation is that there appears to be a higher density of emitted electrons.

Similarly, the beam has flushed all emitted electrons by the end of the simulation, so the neutralization is accomplished entirely by the beam.

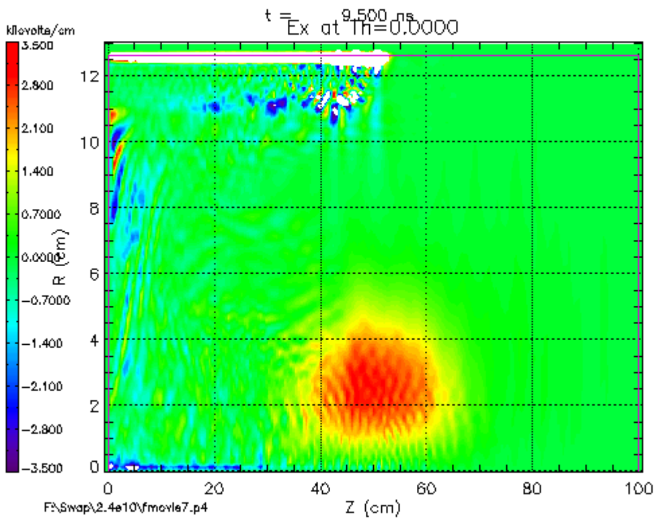

The electric field is still neutralized to 2% of its un-neutralized strength.

The current is still relatively poorly neutralized - 75%, again.

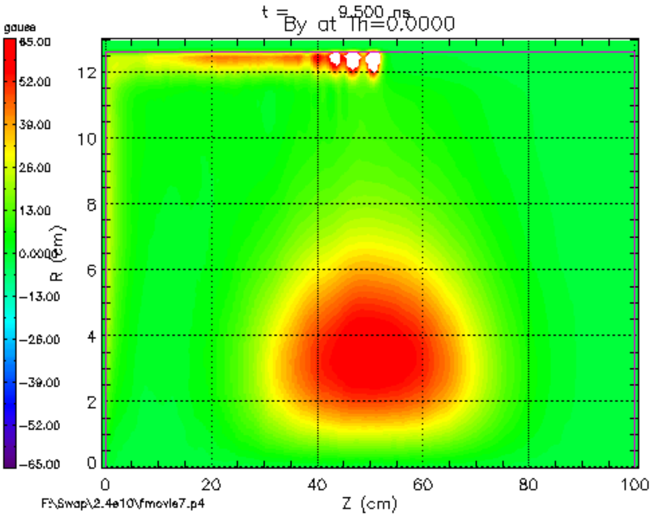

Now, we compare the case where $n_b/n_p = 15$.

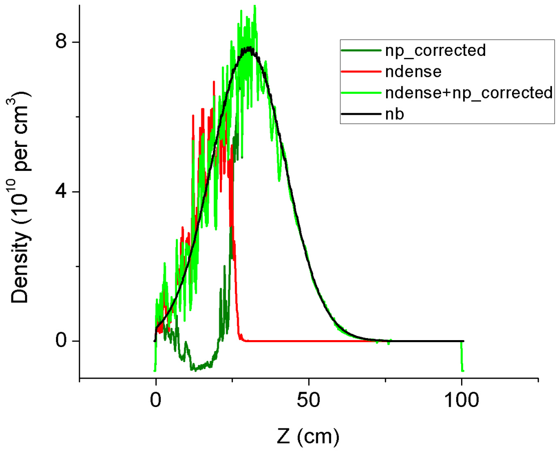

Reliance on emitted electrons is again strong, acting over a range of about 25 cm in the z direction.

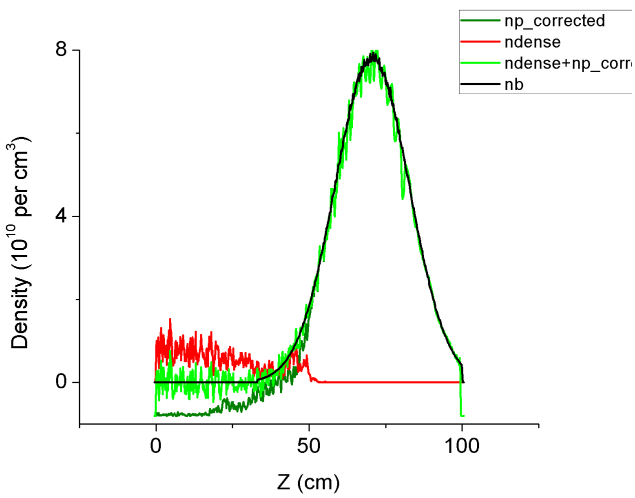

The emitted electrons have been entirely flushed from the beam pulse.

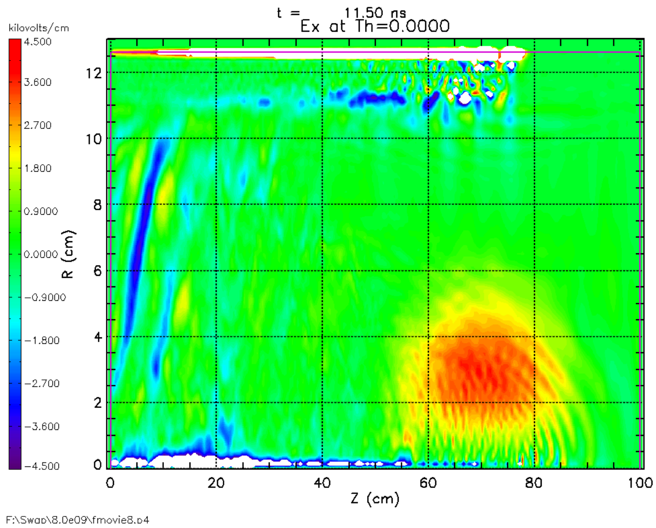

The electric field has been neutralized by more than 98%.

Extremely Weak Plasma

I also investigated the case where $n_b/n_p = 30$, an extremely tenuous plasma, with a dense plasma region on the walls as a secondary electron source.

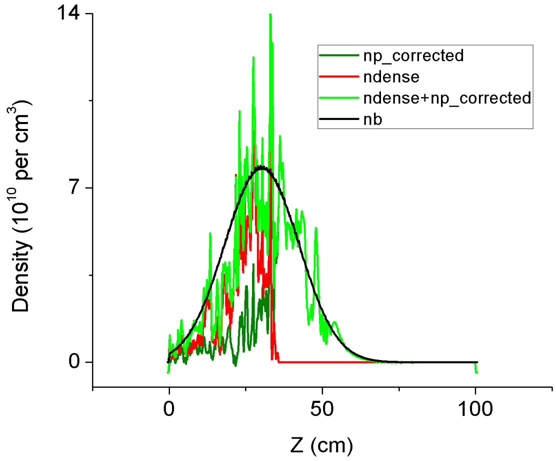

Reliance on emitted electrons is so heavy as to have visibly poor neutralization in the density slices.

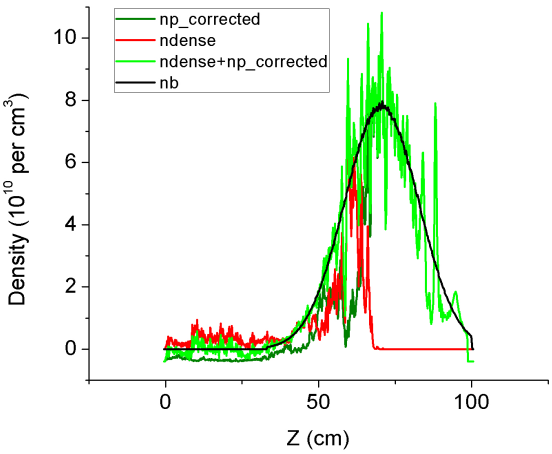

While neutralization has clearly improved, and reliance on emitted electrons from the dense plasma region has lessened, the degree of neutralization is still relatively poor. A longer region of tenuous plasma would be needed to neutralize the beam effectively.

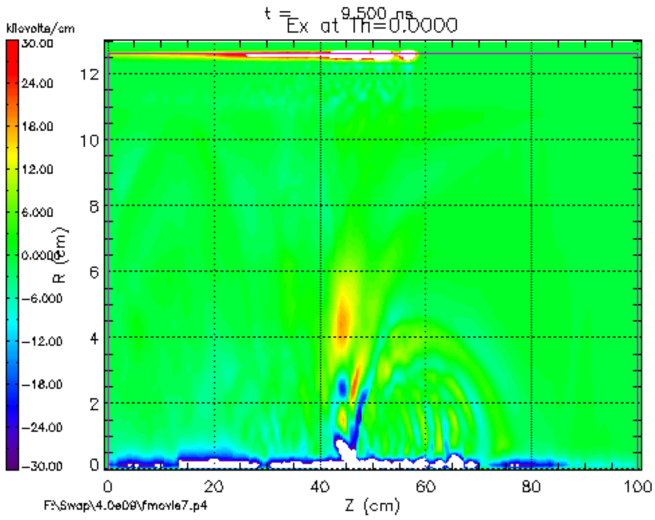

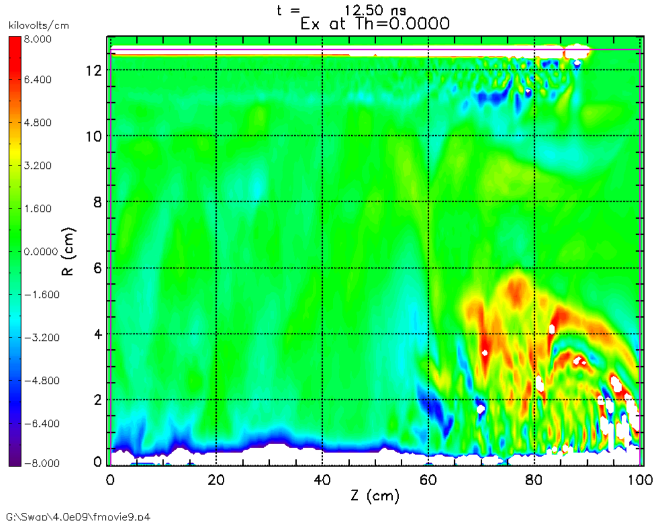

Strong electric fields ~ 30 kV/cm at the early stages of the beam's travel are the result of poor neutralization. However, by the end, the electric fields have been reduced to ~ 8 kV/cm, but the signal is still noisy. This represents 96% neutralization.

CONCLUSIONS

In conclusion, I have numerically demonstrated that even a quite tenuous plasma can neutralize an ion beam pulse effectively given an extra source of electrons. It does not matter the source, as my simulations showed that using Child-Langmuir emitters and a region of dense plasma exhibited the same degree of neutralization. Further, the beam pulls electrons far away, signifying that shielding is almost nonexistent in the cold plasma. Last, the electrons from emitters or dense plasma on the walls helps to neutralize the pulse faster, but they eventually get replaced by cold plasma electrons.

The Princeton Plasma Physics Laboratory is operated
by Princeton University under contract
with the U.S. Department of Energy.

Information Services
Princeton Plasma Physics Laboratory
P.O. Box 451
Princeton, NJ 08543

Phone: 609-243-2245
Fax: 609-243-2751
e-mail: pppl_info@pppl.gov
Internet Address: http://www.pppl.gov